Planar Airfoil Performance

Discussion of the performance (lift and drag) of lifting surfaces, airfoils or wings necessarily begins with an exposition on the steady planar flow of a uniform stream past a two-dimensional airfoil, a flow that is invariant in the direction perpendicular to the plane of the flow, the kind of flow that one would expect at midspan of a wing with very large span. Over the years, beginning with the Wright brothers, extensive wind tunnel tests have been carried out to document the lift and drag on a huge number of designs of two-dimensional airfoils at a series of angles of attack and over a range of Reynolds numbers. A whole catalog of shapes of potential airfoils was maintained by NACA (the precursor to NASA) and can be perused in the book by Anderson (1999). For illustrative purposes, we reproduce in Figures 1 and 2 the measured lift and drag characteristics of two representative airfoils, namely the NACA 23015 and NACA 66_2 215 foils.

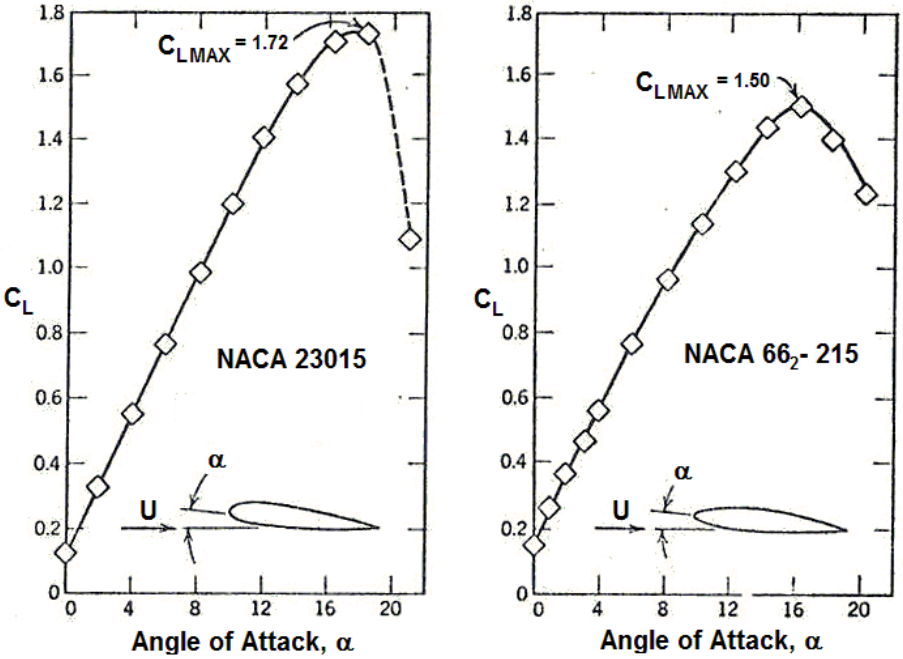

Figure 1: Planar flow lift coefficients as a function of angle of attack for two classic airfoil shapes, the conventional airfoil NACA 23015 and the laminar-flow airfoil NACA 66_2 215.

We begin with comment on the typical lift coefficients shown in Figure 1 and compare these with the lift coefficient, $C_L = 2\pi \sin\alpha$ (or $C_L \approx 2\pi\alpha$), generated by an infinitely thin flat plate at an angle of attack, α, as described in the preceding section. That potential flow solution employed the condition that the flow could not negotiate the sharp trailing edge (the Kutta condition) yet it was assumed that it could negotiate the sharp leading edge. In practice, of course, a real, viscous flow cannot negotiate such a sharp leading edge and therefore practical airfoils are equipped with rounded leading edges in order to induce the flow to remain attached as it rounds the leading edge, at least to the extent that this is possible. However, when the angle of attack exceeds some angle of the order of 12^o no design can prevent separation and stall. In summary an effective airfoil design is one with a rounded leading edge that minimizes separation and a sharp trailing edge that encourages smooth separation.

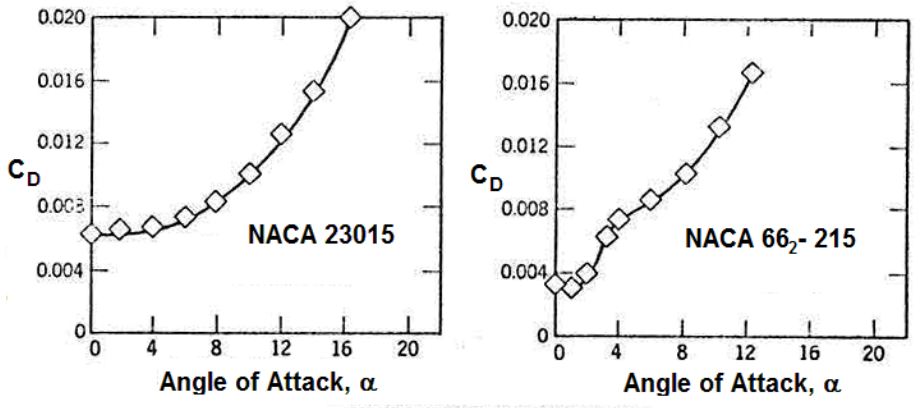

Figure 2: Planar flow drag coefficients corresponding to the lift coefficients of Figure 1.

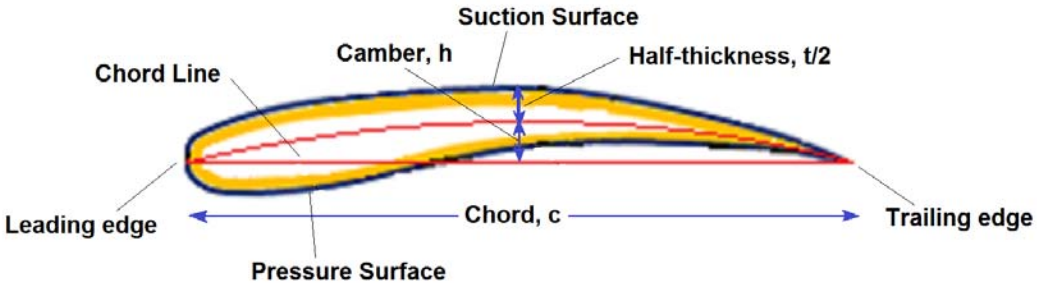

Figure 3: Geometry and terminology of an airfoil.

Focussing on Figure 1 we note that at $\alpha = 8^o$ the NACA 23015 foil generates a $C_L \approx 0.98$ and the $66_2 - 215$ foil generates a $C_L \approx 0.95$ which compare fairly well with $2\pi\alpha = 0.88$. At $\alpha = 12^o$ the corresponding coefficients are approximately 1.4 and 1.3 compared with $2\pi\alpha = 1.32$. Almost all reasonably designed foils at low angles of attack yield lift coefficients close to $2\pi\alpha$, because neither the camber of the foil, h, (see Figure 3) nor the thickness of the foil, t, have a substantial effect on this result. Analyses of the Joukowski solutions for cambered foils show that the lift coefficent for a foil with camber is given approximately by

$$C_L \;\approx\; 2\pi\left\{\alpha + \frac{2h}{c}\right\} \tag{Dce1}$$

Hence the effect of the camber is simply to modify the effective angle of attack; the lift-slope remains unchanged. The effect of a moderate foil thickness is even less and usually amounts to a fractional change in C_L of less than $0.08t/c$. Consequently a value for the lift-slope, $\partial C_L/\partial\alpha$, of 2π is usually a good approximation when α is less than the stall angle. In contrast to the lift, the drag illustrated by the companion graphs of Figure 2 is much harder to estimate analytically and usually has a quadratic-like dependence on the angle of attack like that shown on the left in Figure 2.

In most practical deployments the best performing airfoils are, of course, those with the largest lift but the lowest drag. Thus a graph of the lift plotted against the drag provides a useful way to visualize that performance. Such graphs are called *lift-drag polars* and the lift-drag polar for the foils in Figures 1 and 2 are shown in Figure 4. It follows that to achieve the maximum ratio of lift to drag, L/D, the foil should be operated at the angle of attack, α, corresponding to the point where a line through the origin just touches the lift-drag polar as illustrated in Figure 4 for the NACA 23015 foil. This tangent point defines the angle of attack that yields the maximum value of L/D. Lift-drag polars have other expanded uses. For example if one wished to find the optimal angle of attack when there is additional drag, say from an

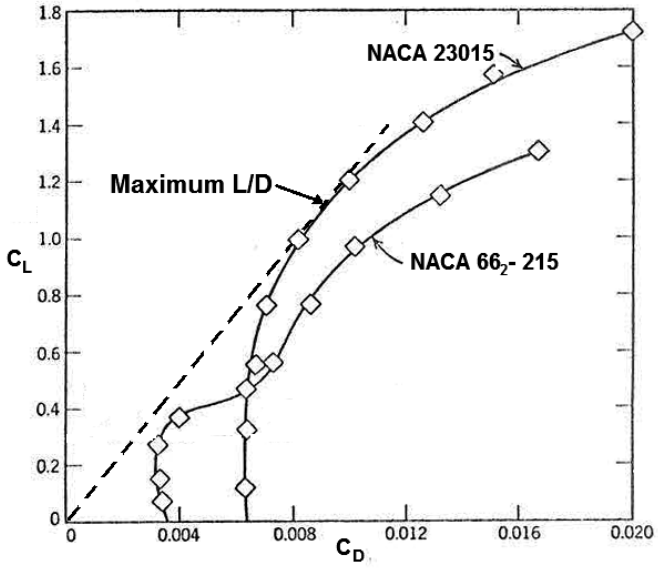

Figure 4: Lift-drag polar from the data of Figures 1 and 2 showing the position of maximum L/D.

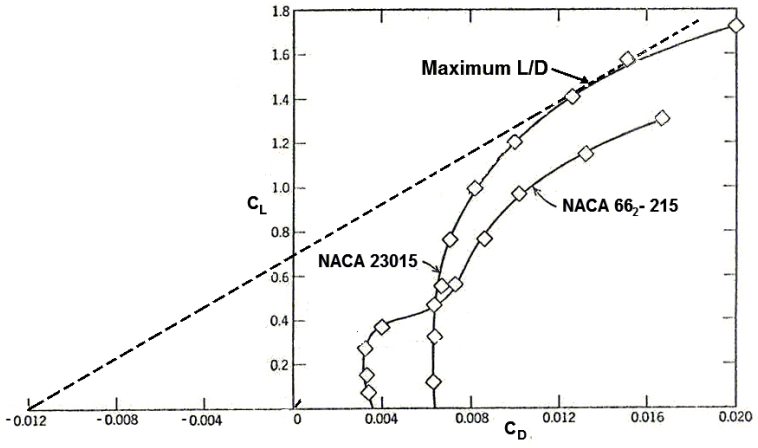

Figure 5: Lift-drag polar from the data of Figures 1 and 2 with position of maximum L/D when additional attached drag is included.

attached fuselage, then that operating point would be given by the line that intersects the horizontal axis at a negative value of C_D (at a negative value given by the drag coefficient of the attached fuselage) and is tangent to the lift-drag polar at a different point and higher angle of attack as exemplified in Figure 5.

When the angle of attack, α, reaches a value that is much dependent on the detailed geometry of the leading edge, the airfoil stalls as the flow separates from near the leading edge and a large separated wake forms behind the foil as illustrated diagrammatically in Figure 6. This begins, usually at an angle of attack of about $\alpha = 15^o$, when the flow separates from the suction surface of the foil. As α increases further the separation point moves forward, approaching the leading edge, and the wake correspondingly expands to dominate the flow behind the foil as illustrated by the flow visualization of Figure 7. As this process of wake expansion proceeds, the associated drag also radically increases. Thus the process of stall is not only associated with a loss of lift but also, and most importantly, with a radical increase in the drag. It is this combination that causes a stalled aircraft to "fall from the sky" as the drag causes a loss of speed which leads to further loss of lift.

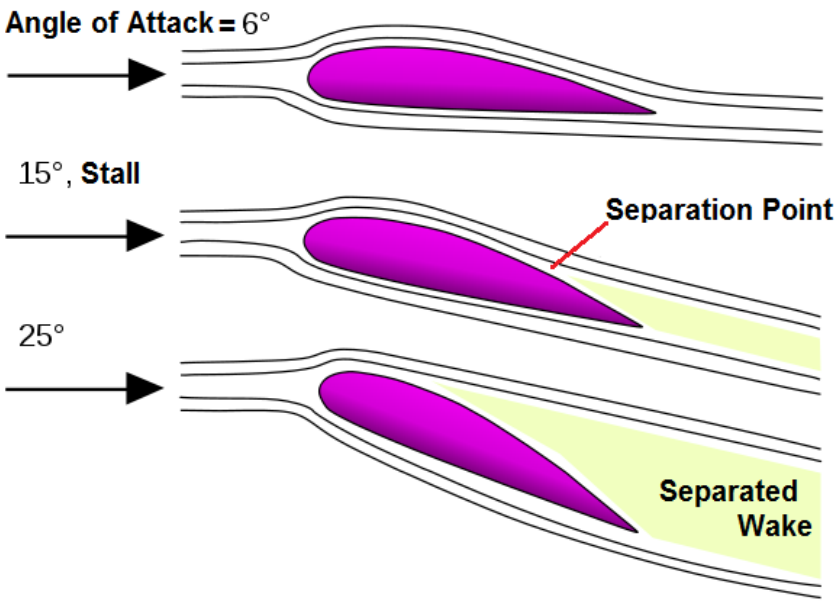

Figure 6: Process of stall in the planar flow around an airfoil.

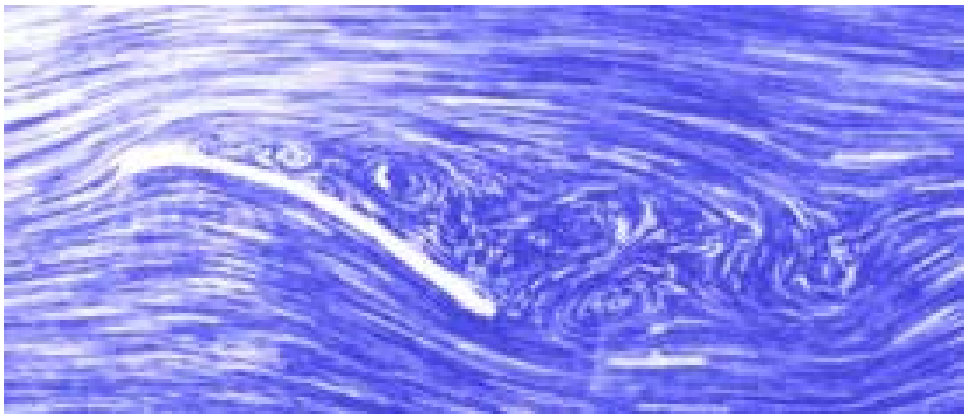

Figure 7: Flow visualization of a stalled airfoil.